LAUNCH COLA GAP ANALYSIS FOR PROTECTION OF THE INTERNATIONAL SPACE STATION

Alan B. Jenkin[(1)], John P. McVey[(2)], Glenn E. Peterson[(3)], Marlon E. Sorge[(4)]

[(1)] The Aerospace Corporation, P.O. Box 92957, Los Angeles, CA 90009-2957, USA, Email: Alan.B.Jenkin@aero.org
[(2)] The Aerospace Corporation, P.O. Box 92957, Los Angeles, CA 90009-2957, USA, Email: John.P.McVey@aero.org
[(3)] The Aerospace Corporation, P.O. Box 92957, Los Angeles, CA 90009-2957, USA, Email: Glenn.E.Peterson@aero.org
[(4)] The Aerospace Corporation, 2155 Louisiana Blvd., NE, Suite 5000, Albuquerque, NM 87110-5425, USA, Email: Marlon.E.Sorge@aero.org

ABSTRACT

For launch missions in general, a collision avoidance (COLA) gap exists between the end of the time interval covered by standard launch COLA screening and the time that other spacecraft can clear a collision with the newly launched objects. To address this issue for the International Space Station (ISS), a COLA gap analysis process has been developed. The first part of the process, nodal separation analysis, identifies launch dates and launch window opportunities when the orbit traces of a launched object and the ISS could cross during the COLA gap. The second and newest part of the analysis process, Monte Carlo conjunction probability analysis, is performed closer to the launch dates of concern to reopen some of the launch window opportunities that would be closed by nodal separation analysis alone. Both parts of the process are described and demonstrated on sample missions.

1 INTRODUCTION

Collision avoidance (COLA) screening is currently performed by requirement for all United States Air Force (USAF) launches [1]. A standard process has been implemented by both the USAF Joint Space Operations Center (JSpOC) and The Aerospace Corporation (Aerospace) [2]. The process determines conjunctions between the launched objects (upper stages and/or satellite payloads) and background objects. The collision probability at these conjunctions is computed based on launch vehicle covariance and compared to a threshold to determine whether a launch opportunity is closed.

The time period covered by the standard launch COLA process extends from launch to 100 minutes after end of launch profile for each of the launched objects. Later times are not considered because the predicted position uncertainty of the launched objects becomes very large. The collision probability becomes diluted so that it cannot exceed established thresholds (e.g., 10^{-6} for manned spacecraft [1]). In addition, the large position dispersion clouds for the launched objects cause the Gaussian/rectilinear theory used to compute collision probability [3, 4] to become invalidated.

The time required for the JSpOC to complete a reliable orbit determination for a launched object depends on the orbit of the object, but in general up to 24 hours may be required. Additional time is then needed to plan and execute collision avoidance maneuvers by other spacecraft and for those maneuvers to achieve clearance. The time period between the end of the time interval covered by the standard launch COLA process and the time that a conjunction involving a launched object can be cleared is known as the COLA gap.

Many missions leave launched objects on orbits that cross the altitude range of the International Space Station (ISS). Special attention is applied to the ISS by the USAF because it is a manned asset. The COLA gap for the ISS is currently considered to last 56 hours. This includes an allowance of 24 hours to complete orbit determination of the launched objects and an allowance of 32 hours for the National Aeronautics and Space Administration (NASA) to plan and execute an ISS evasive maneuver. This accounts for coordination with the Mission Control Center in Russia. A new capability that NASA is developing will make it possible to plan and execute an ISS evasive maneuver within 12 hours, thereby reducing the COLA gap to 36 hours. This capability is currently available for some launch dates.

A COLA gap analysis process has been developed by Aerospace for the USAF Space and Missile Systems Center Launch and Range Systems Directorate (SMC/LR) to address the ISS COLA gap. The analysis process that has been in use until recently consists of two parts: (1) nodal separation analysis, and (2) in-track screening based on a geometric keepout volume. Nodal separation analysis is performed in advance of the launch and identifies launch dates and launch window opportunities that may be closed. In-track screening is performed closer to launch and is intended to open some launch window opportunities that would be closed by nodal separation analysis alone. This process is

Proc. '6th European Conference on Space Debris'
Darmstadt, Germany, 22–25 April 2013 (ESA SP-723, August 2013)

described in [5].

Recently, a Monte Carlo approach has been developed that is intended to replace the geometric in-track screening method in order to reduce conservatism in launch window closures. This new method determines conjunctions using an ensemble of Monte Carlo trajectories for a launched object. These conjunctions are then used to compute collision probability. A new method is used that computes collision probability by estimating a probability density of conjunctions (PDC) in a two-dimensional encounter frame. This method is called the PDC method. The collision probability is then compared to a threshold to determine whether a launch window opportunity is to be closed. The overall method is called Monte Carlo conjunction probability analysis. A related Monte Carlo method for computing collision probability that uses importance sampling was developed by CNES [6].

This paper presents the new COLA gap analysis process. First, the nodal separation analysis is presented and demonstrated on a sample mission (Case 1). After this, the Monte Carlo conjunction probability analysis is presented and demonstrated on two sample missions (Cases 2 and 3). For Cases 2 and 3, collision probability vs. launch window opportunity is computed using the PDC method. Collision probability is also computed via a simple disk intrusion method using both a large disk and a small disk. The three collision probability values are compared. Launch opportunity closures using a sample threshold are evaluated via the three collision probability methods and compared.

Related processes have been developed by the Centre National d'Études Spatiales (CNES) in France [7] and by the NASA Launch Services Program at Kennedy Space Center for NASA launches [8].

2 UPPER STAGE AND ISS TRAJECTORY PROPAGATION

Both the nodal separation analysis and the Monte Carlo conjunction analysis require propagated trajectories of the upper stage and ISS. The Aerospace Corporation's precision integration tool TRACE was used to perform the orbit propagations for the upper stage nominal and dispersion cases as well as for the ISS. This tool was selected because of the need to accurately integrate the upper stage trajectory over 56 hours and the ISS trajectory over weeks to months. For this example case, the force model included the MSIS86 atmosphere model, a 70 x 70 WGS84 Earth gravity model, Sun and Moon gravity, atmospheric drag and solar radiation pressure (assumed reflectivity coefficient = 1.3). To model solar activity, daily and monthly predictions of solar flux parameters F10.7 and the geomagnetic index Ap values were chosen based on when the analysis was performed relative to the launch date. At launch minus six weeks or longer, the 50-percentile monthly predictions are used, which are supplied by NASA Marshall Space Flight Center. An updated analysis is typically performed seven days before launch, and the 45-day daily predictions provided by National Oceanic and Atmospheric Administration (NOAA) are deemed more reliable when the propagation are performed closer to launch.

For the upper stage, the initial conditions are nominal and Monte Carlo dispersion state vectors and vehicle mass at End of Mission (EOM) generated by a launch vehicle trajectory simulation that includes performance and navigation errors. These initial conditions are then propagated over the 56-hour COLA gap period using TRACE.

For the ISS orbit information, the ISS Trajectory Operations and Planning Office at NASA supplies a standard six-week trajectory on a weekly basis. This trajectory contains planned maneuvers. For nodal separation analyses across a launch date range that goes beyond the six-week span of the NASA trajectory, a TRACE trajectory is fit to the NASA trajectory by adjusting the ballistic coefficient, and the resulting fit is propagated farther into the future to cover the launch date range of interest. Trajectory fitting is required to accommodate differences between the propagation theory used to generate the NASA trajectory and the TRACE propagation theory, especially differences in the atmosphere models. The trajectory fitting process is discussed in more detail in [5].

3 NODAL SEPARATION ANALYSIS

The nodal separation analysis computes an approximation to the distance between the orbit traces of the launched object and the ISS, and is used to identify launch dates and launch window opportunities for which those orbits could cross during the COLA gap and may have to be closed. Only the five slowly varying orbital elements are required for this analysis; in-track information is not used. It has typically been performed at launch minus six weeks and then updated at launch minus seven days, although it can be performed as early as launch minus two to three months with sufficient accuracy to identify launch dates and approximate launch window intervals of concern.

A recent mission left an upper stage on a highly eccentric orbit that crossed the ISS altitude range near perigee. This mission had low nodal separation for a range of launch days and is therefore used as an example in this paper to demonstrate the ISS nodal separation analysis (Case 1). For the nodal separation analysis, the upper stage EOM Monte Carlo state vectors were taken from data supplied by the launch vehicle contractor to support the mission. Fig. 1 shows a snapshot of the upper stage dispersion cloud at third perigee pass. For generation of this image, EOM Monte Carlo state vectors supplied by the Aerospace Guidance Analysis Department were used.

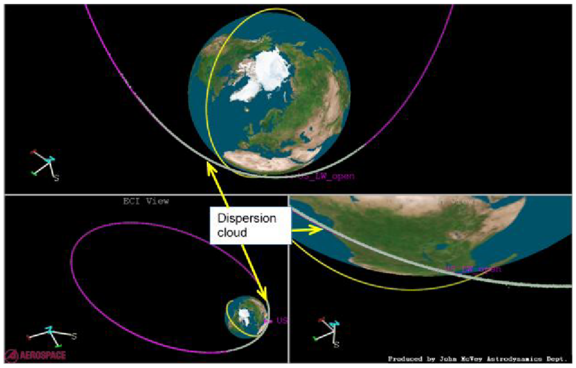

Figure 1. Upper stage position dispersion cloud at third perigee pass for Case 1 example.

The nodal separation between two orbits is defined as the distance between the orbit traces along the line of intersection of the two orbit planes. This is therefore the difference between the orbital radii along the common line of nodes. Fig. 2 illustrates the nodal separation orbital geometry. The nodes for each orbit occur at the orbit points that lie on the common line of nodes. There are always two nodal separation distances, one for each pair of nodes, i.e., one on each side of the common line of nodes. Given the orbital elements for both objects, it is straightforward to compute the nodal separation distance, and no numerical iteration is required. The common line of nodes is obtained from the cross product of the normal vectors of the two orbits. For each orbit, the arguments of latitude at which the radii are computed are determined from the dot product of the unit vector of the common line of nodes and the unit vector of the line of intersection of the orbit plane and equatorial plane. For non-coplanar orbits, each nodal separation distance is a good approximation to the local minimum distance between the orbit traces, which is a lower bound on the conjunction miss distances. For all the missions considered to date, the launched object and ISS orbits have been non-coplanar due to the inclination difference between the two orbits.

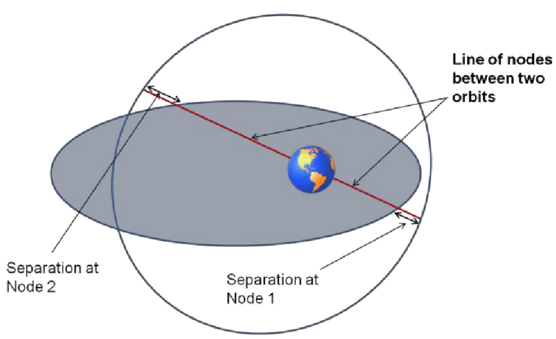

Figure 2. Nodal separation orbital geometry.

When nodal separation is being evaluated for a broad range of launch dates, the following process is used. The nominal upper stage trajectory and a mean ISS trajectory with large (0.5 day) time steps are used for the nodal separation computation. This limits the computation time required to evaluate a broad range of dates. For each launch date and launch window opportunity, the nodal separation distance at each node pair is computed for a range of time points across the COLA gap period. At each time point, the smaller of the two nodal separation values from the two node pairs is retained. The smallest of these nodal separation values across all the COLA gap time points is then retained. This process is repeated for all the points in the launch window, resulting in a table of nodal separation distance vs. launch window opportunity for that launch date. For each launch date, the minimum and maximum nodal separation distances across the launch window are retained.

Figure 3 shows nodal separation vs. launch day across a range of launch days for Case 1. Day 1 corresponds to the first day in the launch date range. On each launch day, a vertical bar is shown. The lowest point on the bar corresponds to the minimum nodal separation across the launch window for that launch day. The highest point on the bar corresponds to the maximum nodal separation across the launch window for that launch day. This analysis was performed approximately six weeks before the first launch day. Days 1 through 7 show low nodal separation.

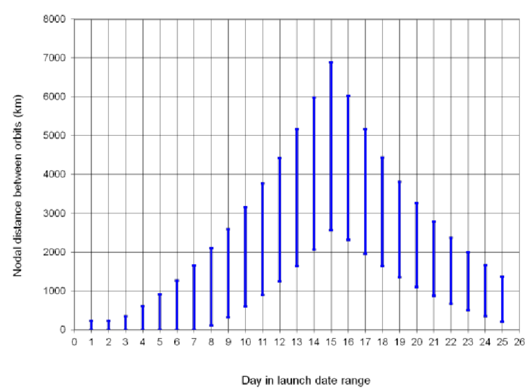

Figure 3. Nodal separation between the ISS and upper stage orbits vs. launch day for Case 1.

Once launch dates with low nodal separation are identified, a more detailed analysis is performed. The same process as described above is executed. However, the nodal separation is evaluated only for COLA gap time points when the upper stage is in the vicinity of the ISS orbit, i.e., the upper stage in-track information is used. An osculating ISS trajectory with small time steps (30 seconds) is used for the nodal separation computation. These two modifications improve the modeling of the effects of short-period trajectory variations near the node pairs. For each launch date, the nodal separation distance vs. launch window opportunity tables are then generated for all the Monte Carlo trajectories. This process is executed on the High Performance Technical Computing cluster at Aerospace using Sun Grid Engine to manage the run jobs. This capability makes it possible to generate an ensemble of nodal separation distance vs. launch window opportunity tables across a range of eight days in approximately five to 10 minutes. From the resulting ensemble of tables, the 99.865-percentile low and high values for each launch window opportunity are computed.

In the nodal separation analysis portion of the process, a launch window minute is considered for closure if the 99.865-percentile low nodal separation is less than 2 km. The 2 km threshold is intended to account for ISS orbit uncertainty. Minutes marked for closure only remain closed if the subsequent Monte Carlo conjunction probability analysis (described in Section 5 of this paper) also indicates closure.

Fig. 4 shows the resulting 99.865-percentile nodal separation vs. launch window plots for Case 1 launch day 3. As the launch days pass, the pattern over the launch window shifts to the left. Nodal separation analysis is discussed in more detail in [5].

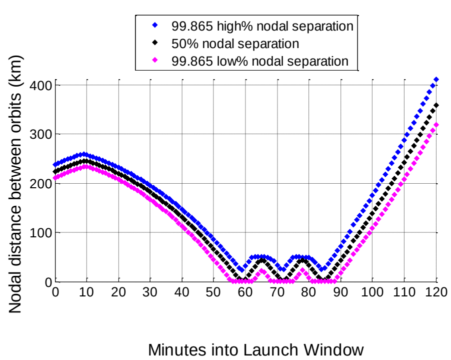

Figure 4. Nodal separation vs. launch window opportunity: Launch Day 3.

4 MONTE CARLO CONJUNCTION PROBABILITY ANALYSIS

The Monte Carlo conjunction probability analysis consists of the following steps. First, 10000 upper stage Monte Carlo EOM state vectors are propagated over the COLA gap period (EOM to EOM+56 hours) using TRACE. Next, conjunctions between the ISS and all of the upper stage Monte Carlo trajectories during the COLA gap period are determined. The probability of collision between the upper stage and the ISS is then computed from the Monte Carlo conjunctions using the PDC method. Probability of collision is compared to a threshold to determine launch opportunity closure.

4.1 Conjunction Generation

A specialized tool was developed to rapidly generate ISS/upper stage conjunctions for each of the Monte Carlo trajectories, which are then used in the probability process to be described in the next section. In normal launch collision avoidance (LCOLA) operations, The Aerospace Corporation's software suite Collision Vision (CV) determines close approaches and probabilities of collision; however, the specific requirements of the COLA gap process make using CV unappealing. Given the length of the COLA gap (up to 56 hours vs. 2-3 hours for nominal LCOLA) and the number of trajectories (10,000), the run times of CV are on the order of several hours. This would normally not be an issue except that the final COLA gap report is due at the L-2 hour point in the launch countdown and the customer desires both the LCOLA and COLA gap processes to use the latest, most up-to-date data possible for this final analysis. This makes it necessary to have quick turn-around times.

In close approach determination between two orbiting objects over a given time span (such as the 56 hour COLA gap), multiple local minimums will occur in the close approach distance function. When one of the objects, such as an upper stage from a launch to geosynchronous orbit, is on a highly elliptical orbit, and the other is in low Earth orbit with a 1-2 hour period, then many of these local minimums will occur when the upper stage is in fact far away from LEO. The main driver in the computation time is the determination of the point of close approach which involves a numerically intensive iterative loop [9, 10]. Therefore, if the numerous iterative loops involving those far away local minimums can be pre-identified and removed from the analysis before actual close approach determination, then significant computation time can be saved.

This pre-identification process consists of sampling the Monte Carlo trajectories and saving three points from each trajectory into one comprehensive file: entry and exit point of the trajectory near-ISS altitude (currently chosen conservatively to be 800 km in altitude) and the corresponding perigee point. It is this arc of each of the upper stage trajectories that is used to determine the close approach point with the ISS. In essence, the search for a close approach is limited to only that portion of each upper stage trajectory that could yield a close approach that is itself close to the ISS.

One of the benefits of this pre-sampling is that the perigee point determination can be performed well in advance of the actual launch date once the Monte Carlo trajectories are generated and are fixed. Updates to the COLA gap analysis during the L-48 hour, L-24 hour, and L-2 hour points therefore become singly reliant upon changes in the ISS trajectory, not the upper stage. For each update that is operationally desired, the ISS trajectory can be updated without disturbing the previous upper stage perigee point determination. This allows for the process during launch countdown to run within minutes rather than hours.

Once the upper stage perigee points are determined, then the close approach conjunctions with the ISS are found. The same software algorithms that are used in CV to find the close approach point are used in the new tool so there is no loss of computational process accuracy. However, it should be noted that some small (meters) level of error is introduced since the close approach algorithm in the new tool starts with the entry and exit points of the upper stage trajectory rather than examining the trajectories on a denser time step-by-time step basis (as in LCOLA). This results in some loss of accuracy being introduced into the close approach interpolation. Since the probability analysis is being performed in a Monte Carlo sense that samples the trajectory uncertainty space, this loss of accuracy is deemed acceptable. The tool can utilize either Earth-centered Cartesian trajectories (which can include planned maneuvers) or two-line element sets to represent the temporally varying position of the ISS.

4.2 Collision Probability

The PDC used to compute the collision probability between the upper stage and ISS consists of the following steps. First, a detection sphere centered on the ISS (usually with a radius of 100 km) is used to select Monte Carlo case conjunctions that will be used for the computation. The selected conjunctions are then mapped into a two-dimensional composite encounter frame. Examples of this frame will be shown for Cases 2 and 3. Next, the probability density of the conjunctions in a smaller region in the encounter frame containing the ISS collision area is computed. The probability of collision is then computed by multiplying the conjunction probability density (PDC) and the ISS collision area (circle with 70 m radius centered at the origin).

To compute the PDC, a rectangular detection box (referred to as the green box in subsequent figures) that contains the ISS collision area is used to further filter down to conjunctions that have an approximately uniform spread in the direction transverse to the long arc of the spread. A second box is determined that is either coincident or inside the first box. It is intended to more tightly fit the conjunction point spread. This box establishes the area used to compute the local PDC and is therefore called the PDC box (referred to as the black box in subsequent figures). The detection and PDC box dimensions are determined adaptively from the conjunction point spread. The PDC box efficiently fits conjunction points (minimizing open spaces and preserving uniform variation of conjunction points inside the box).

If there are a low number of conjunctions inside the PDC box, a bi-variate probability density function (PDF) that is uniform in one direction and Gaussian in the orthogonal direction is determined from the conjunctions selected by the detection sphere. The maximum probability value resulting from the PDC box value and the bi-variate PDF value is then selected for the final result. Including the bi-variate PDF mitigates against conjunction point sparseness.

A simple disk intrusion method has also been proposed for computing collision probability. In this method, the number of conjunctions in a disk centered on the ISS is scaled by the ratio of the areas of the ISS collision cross section and the disk side area (thickness x diameter), and then divided by number of Monte Carlo cases. The disk has the axis of revolution and the thickness dimension parallel to the radius vector from the Earth center to the ISS. Two disk sizes were considered: a large disk (thickness = 20 km, diameter = 100 km) and a small disk (thickness = 4 km, diameter = 50 km). The large disk requires fewer Monte Carlo trajectories. The small disk requires more Monte Carlo trajectories. The advantage of the disk intrusion method is simplicity. The disadvantage relative to the PDC method is that it inefficiently fits conjunction points, leaving many open spaces inside the disk and not accounting for non-uniform variation of conjunction points in the large disk. This method was also implemented for Cases 2 and 3 and results were compared to those of the PDC method.

4.3 Results for Cases 2 and 3

Two recent missions that left upper stages on highly eccentric orbits with low nodal separation are used here as examples to demonstrate the Monte Carlo conjunction probability analysis. Case 2 (the first of the two missions) is similar to Case 1 and has typical dispersion cloud growth. The orbital element dispersions were approximately Gaussian. Case 3 is significantly different from Cases 1 and 2 and has very large, non-Gaussian dispersion cloud growth. Fig. 5 shows a snapshot of the upper stage dispersion cloud at third perigee pass for Case 3. For these two cases, the upper stage EOM Monte Carlo state vectors were supplied by the Aerospace Guidance Analysis Department.

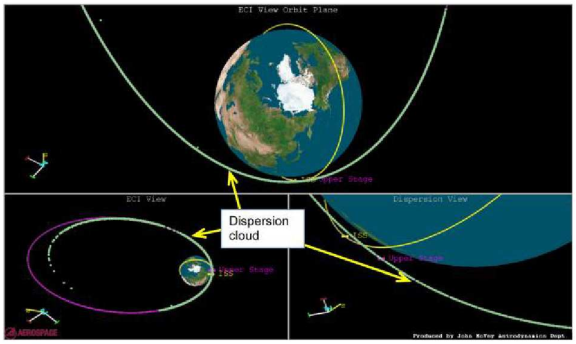

Figure 5. Upper stage position dispersion cloud at third perigee pass for Case 3 example.

Fig. 6 shows upper stage vs. ISS collision probability vs. launch window opportunity for Case 2 Day 1. Results from the simple disk intrusion methods are also shown. In addition, the plot shows the AFI 91-217 threshold for manned objects (10^{-6}) [1] and a threshold that has been proposed for the ISS (10^{-8}). The resulting launch window closures using the 10^{-8} threshold are: 5% from the large disk method, 4.1% from the small disk method, and 3.3% from the PDC method.

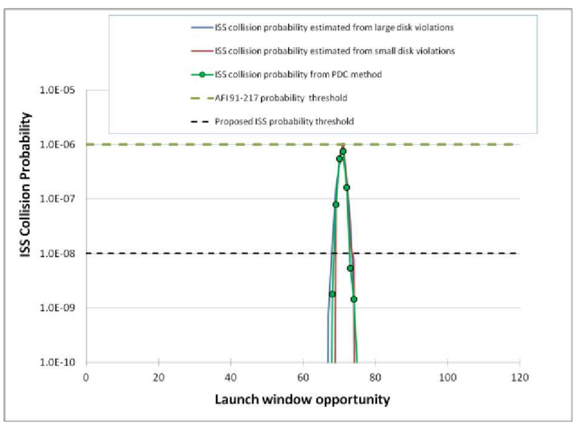

Figure 6. ISS collision probability vs. launch window opportunity for Case 2, Day 1.

Fig. 7 shows Monte Carlo conjunctions within 1000 km for Case 2 with launch on Day 1 at launch window opportunity 69. These conjunctions occur between 13 and 14 hours after EOM. Conjunctions are shown in the ISS radial/in-track/cross-track (RIC) frame. It is seen that the distribution of conjunction points over this large region is curved and not Gaussian (not ellipsoidal).

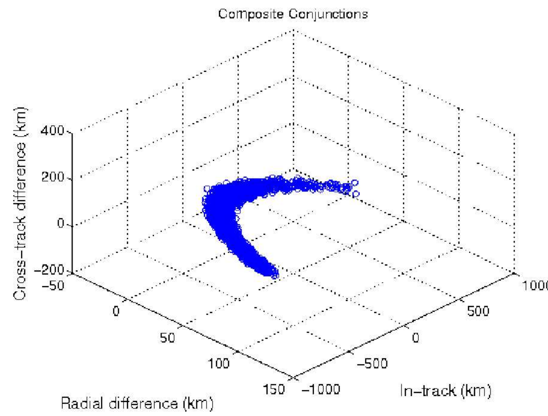

Figure 7. Composite conjunctions in the ISS RIC frame for Case 2, Day 1, launch window opportunity 69.

Fig. 8 shows all conjunctions in a composite encounter frame within a 1000 km detection sphere. In this frame, the origin is at the ISS. For each conjunction, the z-axis (orthogonal to the page) is parallel to the relative velocity vector between the upper stage and the ISS. The y-axis is perpendicular to the inertial velocity vectors of both objects. The x-axis completes the right-handed system. It is seen that the overall distribution is non-Gaussian and non-uniform. However, the variation of point density along the long arc within 100 km of the origin (indicated by the rectangle) is much smaller than the overall variation in the plot. This region is used to compute the collision probability.

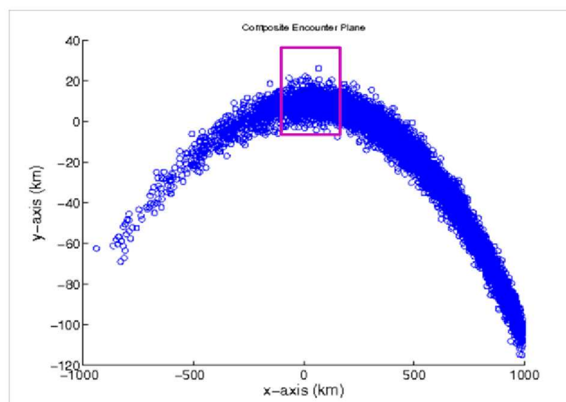

Figure 8. Conjunctions in the composite encounter frame for Case 2, Day 1, launch window opportunity 69.

Fig. 9 shows the conjunctions from Fig. 8 that are within a 100 km detection sphere. It is seen that the curvature of the distribution is not significant, and the variation in point density along the arc is small, thereby motivating the assumption of uniformity of the PDF along the long arc. The magenta lines indicate the 3-sigma boundaries of the conjunction point distribution. The green box is the detection box that selects conjunctions with an approximately uniform transverse spread. The black box is the PDC box and in this case is coincident with the green box. At this launch window opportunity, the resulting PDC collision probability between the upper stage and the ISS is 6.9 x 10^{-8}. In comparison, the large disk ISS collision probability is 1.6 x 10^{-7}, and the small disk ISS collision probability is 7.8 x 10^{-8}.

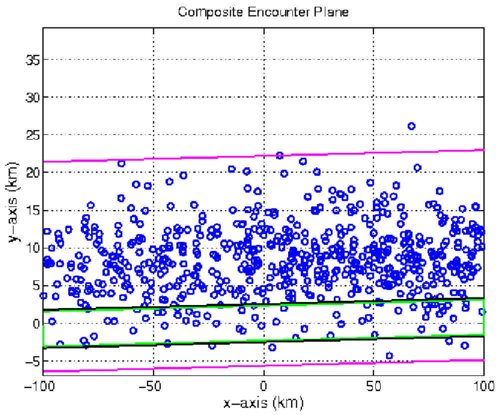

Figure 9. Conjunctions within 100 km in the composite encounter frame for Case 2, Day 1, launch window opportunity 69.

Fig. 10 shows upper stage vs. ISS collision probability vs. launch window opportunity for Case 3 Day 1. The resulting window closures using the 10^{-8} threshold are: 63.8% from the large disk method, 29.8% from the small disk method, and 22.3% from the PDC method. In this case, it is seen that the large disk values are very inaccurate overall. Use of a large disk can significantly over-estimate collision probability, resulting in unnecessary launch window opportunity closures. This over-estimation occurs when the conjunction point distribution is sparse at the origin but not elsewhere in the disk. Use of a large disk can also significantly underestimate collision probability, resulting in failure to show threshold violation. In addition, it is seen that the small disk values are zero for some launch window opportunities for which the PDC values are non-zero. In these cases the small disk method does not account for non-zero conjunction point distribution at the origin. More than 10000 Monte Carlo cases would be needed for the small disk method to yield a non-zero result. The PDC method accounts for both compression of the dispersion cloud and the non-zero conjunction point distribution at the origin.

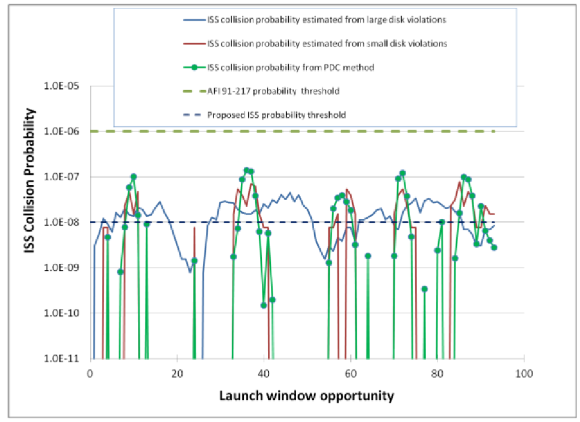

Figure 10. ISS collision probability vs. launch window opportunity for Case 3, Day 1.

Fig. 11 shows Monte Carlo conjunctions that determine the ISS collision probability at launch window opportunity 37 of Case 3 Day 1. These conjunctions occur between 22 and 23 hours after EOM. In this case the black box is inside the green box. The black box more efficiently bounds the point spread and also contains the collision region. At this launch window opportunity, the large disk collision probability is 1.5 x 10^{-8}, the small disk collision probability is 6.9 x 10^{-8}, and the PDC collision probability is 1.3 x 10^{-7}, which is an order of magnitude higher than the large disk result. The large disk value is a significant underestimate because it does not account for the lateral compression (hence higher density) of the dispersion cloud.

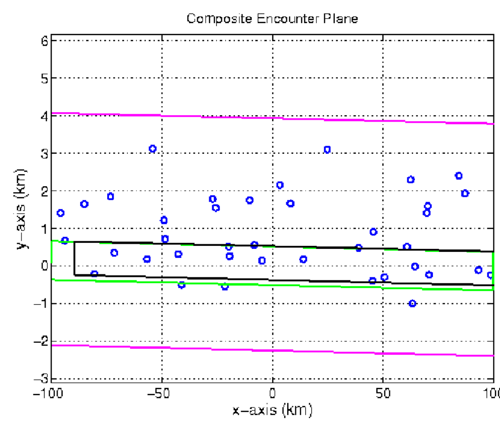

Figure 11. Conjunctions in the composite encounter frame for Case 3, Day 1, launch window opportunity 37.

5 CONCLUSIONS

A new version of the COLA gap analysis process has been developed to address the ISS COLA gap after launch. Nodal separation analysis identifies a range of launch days and launch window opportunities for which the upper stage and ISS orbits could cross during the

COLA gap. Monte Carlo conjunction probability analysis determines window closures on launch days with low nodal separation and is planned to replace the geometric in-track screening process that has been used to data. It uses an efficient method to determine all conjunctions over the COLA gap interval for a set of upper stage Monte Carlo trajectories (currently 10000). It then determines upper stage vs. ISS collision probability via a method that computes the probability density of conjunctions (PDC) in a region containing the ISS.

Simple disk intrusion methods that have been proposed for computing collision probability were compared to the PDC method. It was found that use of a large disk can be very inaccurate for large dispersion cases, resulting in unnecessary launch window opportunity closures as well as failure to show threshold violation. The PDC method is more accurate than use of a large disk because the PDC box used in the method more efficiently fits conjunction distributions. Use of a small disk can be accurate, but it requires many Monte Carlo cases (more than 10000 in this study) to avoid zero values when it should show threshold violation.

Additional testing of the PDC method to confirm accuracy is planned for the future.

As a final note, it should be mentioned that launch window closures depend on mission details and threshold selected, and may be different from those shown for the example cases in this study.

6 ACKNOWLEDGMENTS

This work reflects research conducted under U.S. Air Force Space and Missile Systems Center Contract FA8802-09-C-0001. The authors wish to thank several individuals for their support of this work and assistance in preparing this paper. Technical committee members Gerald Guydan, Bart Lundblad, and Ragini Joshi provided technical review of the paper. Steve Hast provided additional technical review. Gerald Guydan, Bart Lundblad, and Bryan Cooley provided internal programmatic support for this work. The Aerospace Long-Term Capability Development program also provided support for development of the Monte Carlo conjunction probability analysis method. Chris Heidelberger of the Aerospace Guidance Analysis Department provided the Monte Carlo EOM state vectors for Cases 2 and 3. The NASA ISS Trajectory Operations and Planning Office under the lead of Lark Howorth has continuously supported the ISS COLA gap analysis process and provides ISS trajectory predictions on a weekly basis. The Aerospace Corporation's Office of Technical Relations and Capt. Raymond Scholz of the Department of the Air Force, SMC/LRE, provided publication clearance review.

7 REFERENCES

1. Air Force Instruction 91-217,"Space Safety and Mishap Prevention Program," February 18, 2010, accessible at www.e-publishing.af.mil.

2. Gist, R.G. Oltrogge, D.L., "Collision Vision: Covariance Modeling and Intersection Detection for Spacecraft Situational Awareness," Paper No. 99-351, AAS/AIAA Astrodynamics Specialist Conference, Girdwood, Alaska, July 1999.

3. Foster, J.L., Estes, H.S., "A Parametric Analysis of Orbital Debris Collision Probability and Maneuver Rate for Space Vehicles," NASA JSC 25898, August 1992.

4. Chan, F.K., *Spacecraft Collision Probability*, The Aerospace Press, El Segundo, California, 2008, Chapter 3.

5. Jenkin, A.B., McVey, J.P., Peterson, G.E., "ISS Protection Process for the COLA Gap After Launch," Paper No. AIAA 2012-5334, Space 2012 Conference and Exhibition, Pasadena, CA, September 11-13, 2012.

6. Dolado, J.C., Legendre, P., Garmier, R., Revelin, B., Pena, X., "Satellite Collision Probability Computation For Long Term Encounters," Paper No. AAS 11-419, AAS/AIAA Astrodynamics Specialists Conference, Girdwood, AK, July 31- August 4, 2011.

7. Vidal, B., Handschuh, D.A., Wang, C. "Collision Risk at Launch," *Proceedings of the Fifth IAASS Conference 'A Safer Space for a Safer World,'"* SP-699, ESA, January 2012.

8. Hametz, M.E., Beaver, B.A., "A Geometric Analysis to Protect Manned Assets from Newly Launched Objects – COLA Gap Analysis," Paper No. AAS 13-360, 23rd AAS/AIAA Spaceflight Mechanics Meeting, Kauai, Hawaii, February 10-14, 2013.

9. Alfano, S., Negron, Jr., D., "Determining Satellite Close Approaches," *The Journal of the Astronautical Sciences*, Vol. 41, No. 2, April-June, 1993, pp. 217-225.

10. Alfano, S., "Determining Satellite Close Approaches, Part II," *The Journal of the Astronautical Sciences*, Vol. 42, No. 2, April-June, 1994, pp. 143-152.